신경회로망을 이용한 공압구동기의 위치 추종제어에 관한 연구

최 기 홍
한성대학교 산업시스템 공학부
(2000. 7. 14. 접수 / 2000. 8. 16. 채택)

A Study on Tracking Position Control of Pneumatic Actuators Using Neural Network

Gi Heung Choi
Department of Industrial Systems Engineering, Hansung University
(Received July 14, 2000 / Accepted August 16, 2000)

Abstract : Pneumatic actuators are widely used in a variety of hazardous working environments. Any process that involves pneumatic actuation is also recognized as "eco-friendly". In most cases, applications of pneumatic actuators require only point-to-point control. In recent years, research efforts have been directed toward achieving precise position tracking control. In this study, a tracking position control method is proposed and experimentally evaluated for a linear positioning system. The positioning system is composed of a pneumatic actuator and a 3-port proportional valve. The proposed controller has an inner pressure control loop and an outer position control loop. A PID controller with feedback linearization is used in the pressure control loop to nullify the nonlinearity arising from the compressibility of the air. The position controller is also a PID controller augmented with the friction compensation by a neural network. Experimental results indicate that the proposed controller significantly improves the tracking performance.

요 약 : 공압구동기는 다양한 형태의 위험작업 환경하에서 사용되고 있다. 또한, 공압구동기를 적용한 공정은 일반적으로 환경친화적인 것으로 인식되고 있다. 대부분의 경우, 공압구동기는 point to point 제어에 사용된다. 그러나, 최근 공압구동기의 정밀 위치제어에 관한 많은 연구가 수행되고 있다. 본 연구에서는 비례밸브로 구성된 공압구동기의 추종위치제어에 관하여 논의한다. 제안되는 제어기는 압력제어 루프와 위치제어 루프로 구성된다. 공기의 압축성에 기인한 비선형성을 상쇄하기 위하여 되먹임선형화에 의한 PID제어기가 압력제어 루프에 사용된다. 위치제어에는 신경회로망을 사용하여 비선형성을 보상한 PID제어기가 사용된다. 실험결과에 의하면, 제안된 제어기는 공압구동기의 추종성능을 대폭 향상시킬 수 있는 것으로 나타났다.
Key Words : tracking position control, pneumatic actuator, neural network

1. Introduction

Pneumatic actuators are widely used in a variety of hazardous working environments. Typical examples include pressing, forming and welding processes, and collision-free transporting of workpieces. Press operations, for example, require component handling between the presses, and safe gripping, feeding and separating of workpieces to insure the safety of workers. In addition, any process that involves pneumatic actuation is generally recognized as "eco-friendly". In most cases, applications of pneumatic actuators require only point-to-point control. However, new requirements on the ability and capacity of pneumatic system are being generated with the expansion of factory automation.

gihchoi@hansung.ac.kr

Pneumatic actuators have many advantages over other types of actuators due to its light and space saving nature as well as fast but accurate operation. When used on robot arms, the mass moment of inertia can be reduced thanks to their minimal weight. The robot is able to operate faster and with greater precision.

One of the industrial conspicuous trends is the expanding need for pneumatic servo systems that can achieve precise tracking position control. In recent years, research efforts have been directed toward meeting this requirement. Most of them apply pulse width modulation (PWM) control using solenoid valve (van Varseveld, 1997; Jeong, 1997). In order for the PWM control method to be effective, the response of the solenoid valve needs to be fast enough so as not to affect the whole system performance. Therefore, the pneumatic servo system should have several fast valves that have small spools. This requirement not only necessitates a large installation area but complex circuitry, which in turn results in slow response of the actuator. Miyata et al. proposed position control of a pneumatic actuator using pressure control loop (Miyata, 1991). Noritsugu et al. carried out robust control of a pneumatic servo system with PCM digital control valve using pressure control loop (Noritsugu and Takaiwa, 1995).

In this study, a tracking position control method for a pneumatic linear actuator with a 3-port proportional valve is proposed. The nonlinearities associated with compressibility of air, the time delay due to slow propagation of air pressure waves, and the large friction forces in pneumatic actuators make the dynamics of pneumatic position control system rather complex. Consequently, precise position control is usually difficult to perform (Pu and Weston, 1989; Choi, et al, 1998; Lim, et al, 1997). The proposed controller is, therefore, composed of an inner pressure control loop and an outer position control loop. The pressure controller regulates the differential pressure in the cylinder using a nonlinear state model of the compressible fluid flow (Noritsugu and Takaiwa, 1995; Slotine and Li, 1991; Drakunov, et al, 1997; Yang, et al, 1997; Oh, et al, 1999). Works to date have suggested numerous friction compensation methods applicable to pneumatic actuators (Zurada; Amin, et al, 1997; Tafazoli, et al, 1995; Tafazoli, et al, 1998; Friedland and Park, 1992; Russell and Norvig, 1995). The outer position controller proposed in this study includes the friction compensation using the multi-layered perceptron type neural network. The validity of the proposed method is evaluated through experiments.

2. System Model

2.1. Valve Model

Fig. 1 depicts the schematic diagram of the pneumatic valve used in this study. The mass flow rate through the orifice can be expressed as (van Varseveld, 1997)

$$\dot{m} = S\lambda_2 \frac{P_u}{\sqrt{RT}} f\left(\frac{p_d}{P_u}\right) \tag{1}$$

where P_u, P_d, R and T are the pressures at the input and output ports, the gas constant (air: 29.2 $m/°K$) and the absolute temperature, respectively. S is the effective area that changes according to the spool position. It can be regarded as the controlling input to the pneumatic system. The flow function f is defined, respectively, as

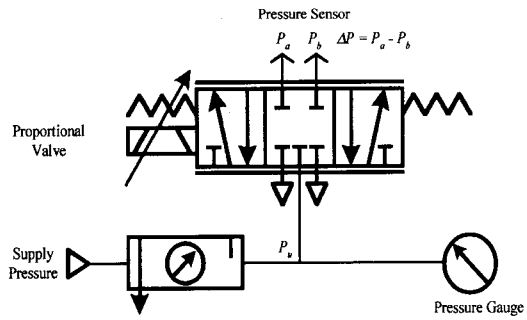

Fig. 1. Schematic diagram of the pneumatic valve used in this study

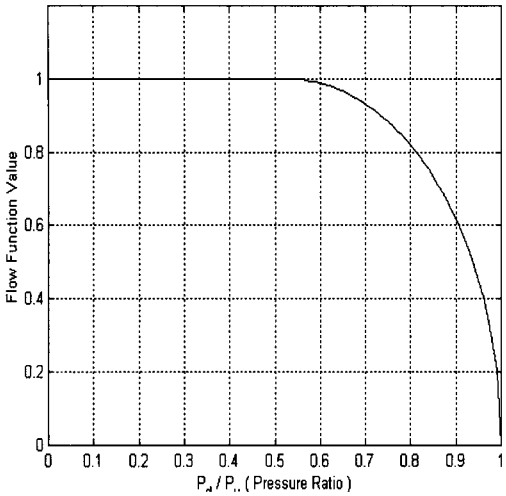

Fig. 2. Variation of flow function with the pressure ratio

$$f\left(\frac{P_d}{P_u}\right)=\begin{cases}\dfrac{\lambda_1}{\lambda_2}\sqrt{\left(\dfrac{P_d}{P_u}\right)^{2/\gamma}-\left(\dfrac{P_d}{P_u}\right)^{(\gamma+1)/\gamma}}, & P_d \geq P_{crit} \\ 1, & P_d < P_{crit}\end{cases} \quad (2)$$

for sonic and subsonic cases, where λ_1 and λ_2 are the dimensionless constants given by

$$\lambda_1=\sqrt{\frac{2\gamma}{\gamma-1}} \quad (3)$$

$$\lambda_2=\sqrt{\gamma\left(\frac{2}{\gamma+1}\right)^{\frac{\gamma+1}{\gamma-1}}} \quad (4)$$

γ is the ratio of the specific heat. In the case of the air, for example, this ratio is 1.4. Fig. 2 shows the variation of flow function with the output-input pressure ratio P_d/P_u.

2.2. Cylinder Model

Assuming isentropic thermodynamic behavior of the air, the following equation is applicable to each chamber

$$P\left[\frac{V}{m}\right]^{\gamma}=\text{constant} \quad (5)$$

where P, V and m are pressure, volume, and mass of the air in the cylinder. Differentiating Eq.(5) with respect to time, one can have

$$\dot{P}\left[\frac{V}{m}\right]^{\gamma}+P\gamma\left[\frac{V}{m}\right]^{\gamma-1}\left(\frac{\dot{V}}{m}-V\frac{\dot{m}}{m^2}\right)=0 \quad (6)$$

or

$$\dot{P}V+\gamma P\dot{V}=\gamma\left(\frac{\dot{m}}{m}\right)PV \quad (7)$$

By substituting the ideal gas law ($PV=mRT$) into Eq.(7) and differentiating, the relationship between the pressure in the cylinder and the rate of mass flow into the cylinder can be obtained as

$$\dot{P}V+\gamma P\dot{V}=\gamma\dot{m}RT \quad (8)$$

Next, the time rate of differential pressure can be written as

$$\Delta\dot{P}=\dot{P}_a-\dot{P}_b=\frac{\gamma\dot{m}_aRT}{V_a}-\frac{\gamma\dot{m}_bRT}{V_b}+\frac{\gamma P_a\dot{V}_a}{V_a}-\frac{\gamma P_b\dot{V}_b}{V_b} \quad (9)$$

and the dynamics of cylinder motion is described by the equation

$$A\Delta P=A(P_a-P_b)=m\frac{d^2x}{dt^2}+f_{fric} \quad (10)$$

where A, f_{fric}, $\triangle P$, P_a and P_b are the cross-sectional areas of the piston, frictional force, differential pressure and pressure in chamber a and in chamber b, respectively.

3. Pressure Controller Design

Fig. 3 shows the block diagram of the overall control system composed of an inner loop pressure control and an outer loop position control. For pressure control, a proportional valve that converts an analog electrical input signal into appropriate

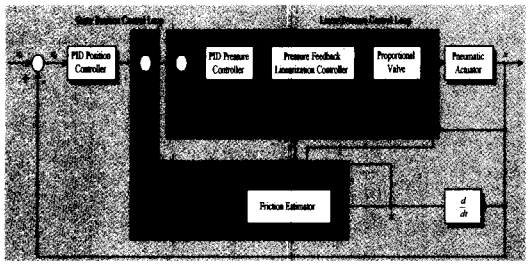

Fig. 3. Schematic diagram of position controller using friction estimator

cross-sectional opening, is used. The differential pressure in the cylinder is directly controlled by the flow rate through the valve. The flow rate is influenced by the input voltage in a complex way. The experimental studies carried out so far have confirmed that the relationship between the cross-sectional areas of port and port b is given by

$$S_b = -K_S S_a \tag{11}$$

where K_S is the proportionality constant. Note that the negative sign in Eq.(11) is introduced to signify the direction of air flow. S_a has the negative value if the air flows in the direction from port b to port a. Suppose that the air flows into chamber a through port a and out of chamber b through port b in the valve. To account for each rate of mass flow, Eq.(1) can be rewritten as

$$\dot{m}_a = S_a \lambda_2 \frac{P_s}{\sqrt{RT}} f\left(\frac{P_a}{P_s}\right) \tag{12.a}$$

$$\dot{m}_b = S_b \lambda_2 \frac{P_b}{\sqrt{RT}} f\left(\frac{P_e}{P_b}\right) \tag{12.b}$$

where P_S is the pressure supplied and P_e is the atmospheric pressure. If the air flows in the reverse direction, the equations for mass flow rate take the form

$$\dot{m}_a = S_a \lambda_2 \frac{P_a}{\sqrt{RT}} f\left(\frac{P_e}{P_a}\right) \tag{13.a}$$

$$\dot{m}_b = S_b \lambda_2 \frac{P_s}{\sqrt{RT}} f\left(\frac{P_b}{P_s}\right) \tag{13.b}$$

From Eqs.(12) and (13), the time rate of change of differential pressure in the cylinder can be written as

$$\Delta\dot{P} = \dot{P}_a - \dot{P}_b = \psi_1 S_a + \psi_2 \tag{14}$$

where

$$\psi_1 = \begin{cases} \dfrac{\gamma\lambda_2 P_S f_a \sqrt{RT}}{V_a} + \dfrac{K_S \gamma\lambda_2 P_b f_b \sqrt{RT}}{V_b}, & S_a \geq 0 \\ \dfrac{\gamma\lambda_2 P_a f_a \sqrt{RT}}{V_a} + \dfrac{K_S \gamma\lambda_2 P_S f_b \sqrt{RT}}{V_b}, & S_a < 0 \end{cases} \tag{15}$$

$$\psi_2 = -\frac{\gamma P_a \dot{V}_a}{V_a} + \frac{\gamma P_b \dot{V}_b}{V_b} \tag{16}$$

If the input to the system (the cross-sectional area of the valve, S_a) is set to be

$$S_a = \left(\Delta\dot{P}_r - K_e\left(P_a - P_b - \Delta P_r\right) - \psi_2\right)/\psi_1 \tag{17}$$

the dynamics of the pressure control system becomes linear as described by

$$\dot{e}_{\Delta P} + K_e e_{\Delta P} = 0 \tag{18}$$

where $e_{\Delta P} = \Delta P - \Delta P_{ref}$ and K_e is a constant.

4. Design of Position Controller Using Neural Network

The friction is another important nonlinearity that any pneumatic position control system inherently exhibits. Thus, a controller that can estimate and compensate for friction is critical for precise position control of pneumatic system. Since the differential pressure drives the pneumatic actuator, the pneumatic actuator can be regarded as a system with the differential pressure as the input

and the position as the output. The equation of motion for such an actuator was given in Eq.(10) where the friction term has the following generic form to account for both static and dynamic components:

$$A\Delta P = m\ddot{x} + f_{fric}(\dot{x}, \ddot{x}) \tag{19}$$

In position control of the pneumatic actuators, the performance of a PID controller tends to be unpredictable and unsatisfactory, mainly due to the inherent friction. In order to compensate for the friction, the friction estimator based on a neural network is introduced in the outer loop PID position controller. In the friction estimator, the input voltage corresponding to the measured output velocity and acceleration is calculated using the friction model coded on the neural network. To encode the relationship between the actuator velocity and acceleration, and the friction force, a 2-3-1 multi-layered back propagation neural network shown in Fig. 4 is used.

Referring to Fig. 4, each neuron in the network forms a weighted sum of the inputs from the previous layer to which it is connected, adds a bias value, and produces an output which is a nonlinear function of this sum according to the following relationship:

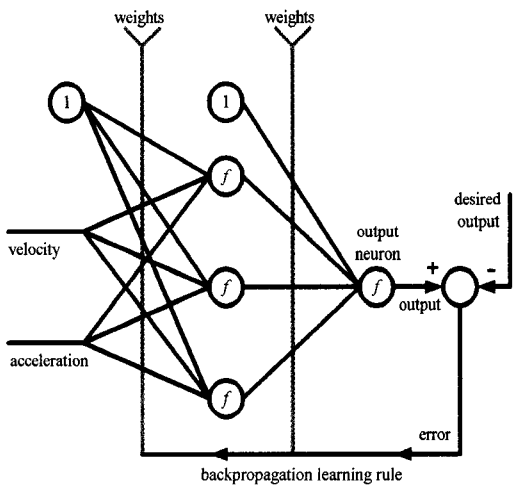

Fig. 4. The 2-3-1 back propagation neural network used in this study

$$net_{i,k} = \sum_j w_{i,j,k} O_{j,k-1} + t_{i,k} \tag{20}$$

$$O_{i,k} = \frac{1}{1+e^{-net_{i,k}}} \tag{21}$$

where

$net_{i,k}$: input to i^{th} node in the k^{th} layer

$O_{i,k}$: output of i^{th} node in the k^{th} layer

$w_{i,j,k}$: weight between j^{th} node in k^{th} layer to i^{th} node in k^{th} layer

$t_{i,k}$: threshold of the i^{th} node in the k^{th} layer

This output along with other outputs from the neurons in the same layer serve as the input to the next layer, and the process is repeated. The back propagation algorithm is used to adjust the weights and bias during encoding of the input/output relationship of training samples. To overcome slow training speed and local minimum problem of the back propagation rule, adaptive learning rate (Tafazoli, 1995) is used.

In the operation mode, the compensating signal, which counterbalances the friction, is calculated from the neural network model, and used to cancel out the friction. With the friction compensation the overall dynamics can be assumed linear if the modeling error is small enough to be ignorable. In such cases the dynamics of the actuator can easily be controlled by adjusting the parameters of the outer loop PID controller.

5. Experiments

The experimental setup used is shown in Fig. 5. A linear positioner (Festo, LA-200) which consists of a slide, a double-acting rodless cylinder, two guide rods, end stops and two end plates is set horizontally and is driven by pneumatic cylinder. The weight of the slide is 2.7kg, and the diameter and the stroke of the pneumatic cylinder are 25mm and 200mm, respectively. The 3-port proportional control valve, which operates at 600kPa(Festo, MPYE-5-1/8), was used. The proportional control valve can adjust the flow-rate from -700*l*/min to 700*l*/min

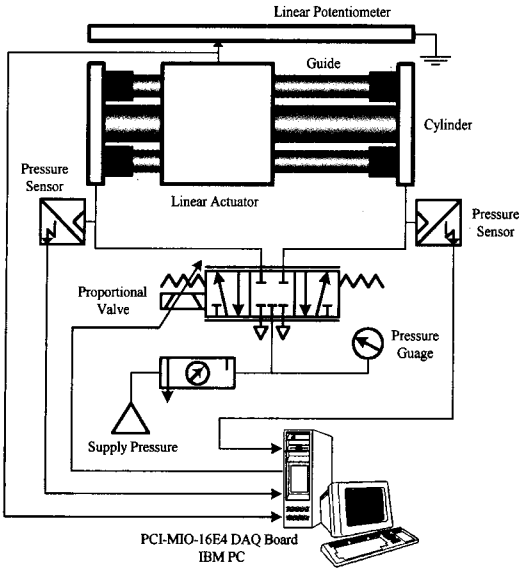

Fig. 5. Experimental setup used in the experiment

in accordance with the input voltage (0 to 10V) by changing the spool position. The system bandwidth was set at 10Hz. When the input voltage is half the nominal value, i.e., 5 volts, all control edges are closed so that the flow rate is zero. To detect differential pressure between left and right chambers, two pressure sensors (Festo, SDE-10) with the linearity of less than 1% of the full-scale were employed. For the position feedback, a linear potentiometer with the resolution of 1.25μm was employed. It outputs electrical signal proportional to the position. The sensor output is passed to a PC through a data acquisition and control board (National Instrument, PCI-MIO-16E4). The control input is computed by the PC and passed to the 3-port proportional valve using the D/A capability of the data acquisition and control card. The servo rate of the system was set at 100Hz.

6. Results and Discussion

6.1. Pressure Control

The proportional valve used in this study converts an input voltage into a cross-sectional opening. A set of experiments was conducted to estimate the relationship between the input voltage

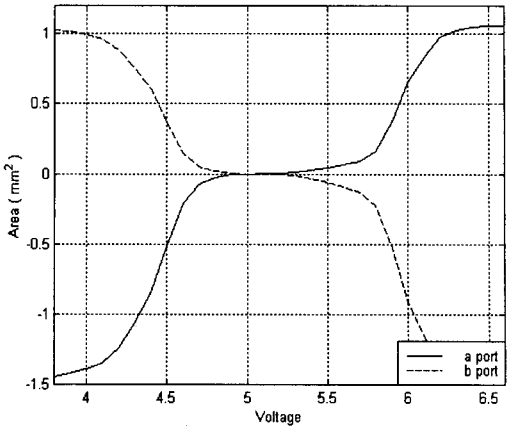

Fig. 6. Estimated cross-sectional area of the proportional valve as a function of input voltage

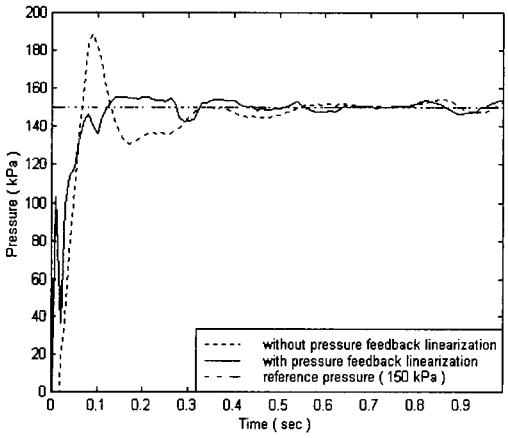

Fig. 7. Experimental result of pressure control

and the effective cross-sectional area. The result was recorded, and used for calculating the input voltage that corresponds to the desired cross-sectional area of the proportional valve. The calculated area as a function of the input voltage is shown in Fig. 6.

Fig. 7 shows the experimental results of a pressure control using the proposed controller based on feedback linearization. The overshoot in the transient response of the uncompensated system is mainly due to the compressibility of the air. The figure indicates that the overshoot can be effectively eliminated by the proposed pressure controller. Consequently, the pressure control performance is substantially improved compared to a simple PID controller.

6.2. Friction Compensation Using Neural Network

The proposed position controller includes the real-time friction estimator based on neural network. The 2-3-1 multi-layered perceptron type neural network is used as the estimator. The parameters of the network is adjusted using training samples, based on the back-propagation learning rule. The actual friction in Eq.(19) was estimated using the measured differential pressure and the acceleration, and used for preparing training samples. Fig. 8 shows the functional relationship between velocity, acceleration, and friction force as obtained from simple tests. The experimental relationship in the figure exhibits the typical characteristics of Coulomb friction. It must be, noted, however, that a slight influence of acceleration, which accounts for the dynamic effects, is also seen in the figure. This information was then coded on the neural network for the subsequent friction compensation.

Fig. 9 shows the learning performance of the neural network, i.e., the difference between the computed disturbance and the actual disturbance. The figure indicates that the 2-3-1 multi-layered perceptron type neural network used in this study was able to effectively simulate such relationship. Ignoring the non-linearity and the higher order dynamics due to modeling error and applying the ARMAX model, the pulse transfer function of the friction compensated actuator was identified as

$$G_s(z^{-1}) = \frac{10^{-3}(0.1892z^{-1} + 0.1875z^{-2})}{1 - 1.9726z^{-1} + 0.9726z^{-2}} \quad (24)$$

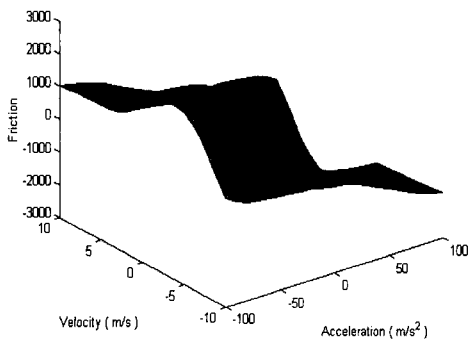

Fig. 8. Estimated friction using neural network

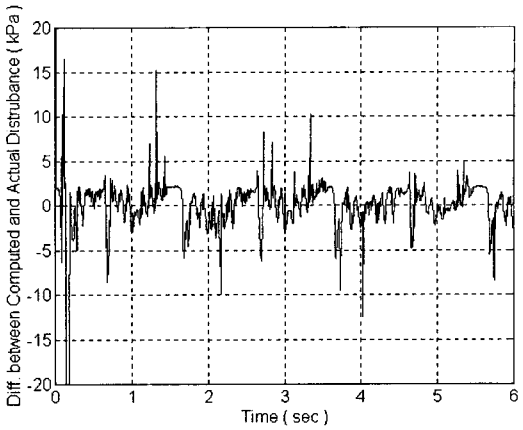

Fig. 9. Difference between the computed disturbances (friction) and the actual disturbances

In tracking position control experiments sinusoids with the magnitudes of 30-70mm, and frequencies of 0.1-0.5Hz were used as reference inputs. The PID control gains for the position control loop were selected such that they minimize the RMS tracking error. They were set at: K_P=12.3, K_I=1.2 and K_D=20.5. Fig. 10 shows the tracking performance of the controller when the reference input is a sinusoid with amplitude of 70mm and frequency of 0.2Hz. In Fig. 10, (a), (b) and (c) compare the tracking performances of controllers with and

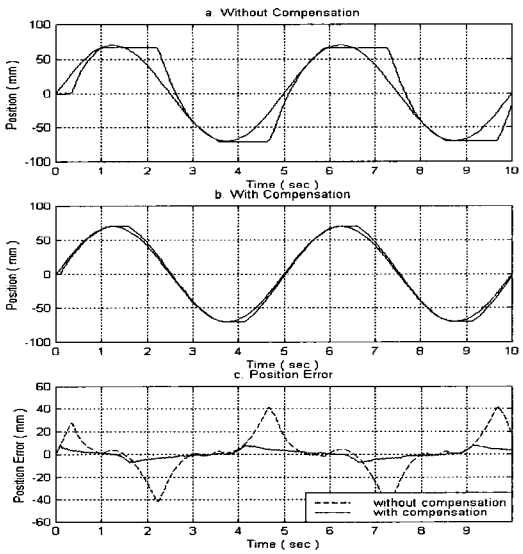

Fig. 10. Experimental result of the controller using neural network

Table 1. Tracking performances of position controller based on neural network for sinusoidal inputs with various amplitudes. Frequency was 0.2

Amplitude (mm)	Peak Error (mm)		RMS Error (mm)	
	Uncompensated	Compensated	Uncompensated	Compensated
30	27.0	6.6	8.8	2.1
40	32.7	7.0	9.5	2.2
50	29.3	7.5	9.6	2.4
60	36.0	7.5	11.5	2.6
70	45.1	8.1	12.1	2.9

Table 2. Tracking performances of position controller based on neural network for sinusoidal inputs with various frequencies. Amplitude was 70

Frequency (mm)	Peak Errors(mm)		RMS Errors(mm)	
	Uncompensated	Compensated	Uncompensated	Compensated
0.1	32.5	7.8	7.0	1.7
0.2	45.1	8.1	12.1	2.9
0.3	25.9	10.6	16.2	4.5
0.4	32.2	13.1	19.2	5.9
0.5	32.4	15.6	20.1	7.3

without the friction compensation. As expected, typical characteristic of the friction near the corner is seen without compensation in the figure. The tracking error, however, drastically decreases with friction compensation. Table 1 summarizes peak and RMS errors for inputs with various amplitudes, whereas performances for inputs with various frequencies are given in Table 2. Maximum reduction of 80% in the peak error and 75% in the RMS error is noticed. If the model of dynamic nonlinearity due to the compliance is identified and incorporated into the feedback linearization, and if the noise arising from differentiating the position is eliminated by directly measuring the velocity, further improvement in the tracking accuracy may be expected.

7. Summary and Conclusion

In this study, a tracking position controller for pneumatic actuators was proposed and experimentally evaluated. The proposed controller has an inner pressure control loop and an outer position control loop. A PID controller with the feedback linearization is used in the pressure control loop to nullify the nonlinearity arising from the compressibility of the air. The position controller is also a PID controller augmented with a friction compensation feature based on the neural network. The nonlinearity due to the friction coded on the neural network in the training mode was used to calculate the proper input voltage that counterbalances the inherent friction in the operation mode. This input voltage is used to cancel out the friction and to linearize the plant dynamics. The experimental results indicate that the tracking performance can be significantly improved with the proposed controller. Specifically, up to 80% reduction in the peak error and 75% in the RMS error is attained.

Acknowledgment : This work was financially supported in part by Hansung University in the year of 1999.

References

1) van Varseveld, Robert B., and Bone, Gary M., 1997, "Accurate Position Control of a Pneumatic Actuator Using On/Off Solenoid Valves," IEEE Transactions on Robotics and Automation, pp. 1196~1201.
2) Jeong, H. S., 1997, "A Study on the Pressure Control Characteristics of On/Off 3-way Solenoid Valve Driven by PWM Signal," Trans. KSME, Vol. 21, No. 3, pp. 485~501.
3) Miyata, K., 1991, "Control of Pneumatic Drive Systems by Using PCM Valves," Flucome '91, pp. 373~378.
4) Noritsugu, T., and Takaiwa, M., 1995, "Robust Position Control of Pneumatic Servo System with Pressure Control Loop," IEEE Transactions on Robotics and Automation, pp. 2613~2618.
5) J. Pu and R. H. Weston, 1989, "A New Generation of Pneumatic Servos for Industrial Robots," Robotica, Vol. 7, No. 1, pp. 17~23.
6) Choi, Gi S., Lee, Han K., and Choi, G. H., 1998, "A Study on Tracking control of Pneumatic Actuators Using Neural Network," Proc. 24th

Annual Conference of the IEEE Industrial Electronics Society, Aachen, Germany, 1998, pp. 1749～1753.
8) Lim, S., and Eao, Y. B., 1997, "Position Servo Control of a PR Type Pneumatic Manipulator," Trans. KSME, Vol. 21, No. 10, pp. 1619～1625.
9) Slotine, E. and Li, W., 1991, Applied Nonlinear Control, Prentice Hall.
10) Drakunov, S., Hanchin, G. D., Su, W. C., and Ozguner, U., 1997, "Nonlinear Control of a Rodless Pneumatic Servoactuator, or Sliding Modes versus Coulomb Friction," Automatica, Vol. 33, No. 7, pp. 1401～1408.
11) Yang, U. K., et al, 1997, "Pressure Control of Hydraulic Servo System Using Proportional Control Valve," Trans. KSME, Vol. 21, No. 8, pp. 1229～1240.
12) Oh, I., et al, 1999, "A Study on the Improvement of the Load Pressure Feedback Mechanism of the Proportional Pressure Control Valve," KSME Int. J., Vol. 13, No. 1, pp. 34～41.
13) Zurada, M., Introduction to Artificial Neural Systems, PWS Publishing, p. 185.
14) Amin, J., Friedland, B., and Harnoy, A., 1997, "Implementation of a Friction Estimation and Compensation Technique," IEEE Control System Magazine, Vol. 17, No. 4, pp. 71～76.
15) Tafazoli, S., Silva, C. W., and Lawrence, P. D., 1995, "Friction Estimation in a Planar Electrohydraulic Manipulator," Proceedings of American Control Conference, Vol. 5, No. 4, pp. 3294～3298.
16) Tafazoli, S., Silva, C. W., Lawrence, P. D., 1998, "Tracking Control of an Electrohydraulic Manipulator in the Presence of Friction," IEEE Transactions on Control Systems Technology, Vol. 6, No. 3, pp. 401～411.
17) Friedland, B., and Park, Y. J., 1992, "On Adaptive Friction Compensation," IEEE Transactions on Automatic Control, Vol. 37, No. 10, pp. 1609～1612.
18) Russell, Stuart J., and Norvig, Peter, 1995, Artificial Intelligence - A Modern Approach, Prentice Hall, pp. 3294～3298.